Organisation and reactivity of silicon-based hybrid materials with various cross-linking levels

Bruno Boury, Robert J. P. Corriu* and Hironobu Muramatsu

Laboratoire de Chimie Moléculaire et Organisation du Solide (CNRS UMR 5637), Université Montpellier II, Place E. Bataillon, 34095 Montpellier cedex 5, France

Received (in Strasbourg, France) 17th October 2001, Accepted 11th February 2002
First published as an Advance Article on the web 8th July 2002

Nanostructured silicon-based hybrid materials were prepared by sol-gel hydrolysis/polycondensation of $(MeO)_{3-n}SiMe_n$–C≡C–C_6H_4–C≡C–$SiMe_n(OMe)_{3-n}$ ($n = 0, 1, 2$) precursors. Their organisation was evaluated by birefringence measurements (microscopy under polarised light) and evidences the possibility of self-association of the macromolecular units in the sol step and reorientation processes in the ageing step. In contrast to the texture (porosimetry with N_2), the cross-linking level of the Si–O–Si network of the solids (^{29}Si CPMAS spectroscopy) appears to be determinant for the anitropic organisation. For $n = 2$ the corresponding polymer –(–O–$SiMe_2$–C≡C–C_6H_4–C≡C–$SiMe_2$–)– is crystallised and demonstrates the strong ability of the organic units to self-associate. This is also suggested by partial polymerisation of the acetylenic moieties of the organic units in the solid state up to 350 °C (DSC, IRTF).

The chemistry of organic–inorganic hybrid materials provides the chemist with interesting possibilities for building new materials. Most of them can be prepared by a one-step inorganic polymerisation sol–gel process, particularly in the case of silicon-based materials. Using precursors with the general formula $R[SiX_3]_n$ ($n \geqslant 2$ and X = OMe, OEt, H, Cl, ...) hydrolysis/polycondensation leads to nanostructured solids according to eq. (1):

$$1\ R{-}[Si(OR)_3]_x + 3/2X\ H_2O \xrightarrow[\text{Catalyst}]{\text{Solvent}} R{-}[SiO_{1.5}]_x + 3X\ ROH \quad (1)$$

The interest of this approach has already been demonstrated,[1–5] and it leads to *inter alia* NLO materials,[6,7] luminescent materials,[8–11] thin films with high dielectric constants,[12] or solids like mesoporous MCM materials.[13,14]

Previous studies have been focused on understanding the formation of these solids in order to control their chemical, structural and textural characteristics. Contrary to silica, which is always amorphous when prepared by the sol–gel method, the possibility of self-organisation in these hybrid materials has been demonstrated by using very specific precursors like octadecyltrichlorosilane,[15] chiral diureidocyclohexane[16] or a bisurea-based precursor.[17] In these specific cases, materials are organised over a long-range scale. Our work has focused on the anisotropic organisation of the solids prepared from rigid precursors, their organisation being described in terms of a short-range order (Scheme 1).[18,19] Furthermore, it was demonstrated that a rigid rod-like geometry for the organic group is best suited to achieve such anisotropic organisation.[20] It was also demonstrated that these phenomena are highly dependent on the experimental parameters used for the sol–gel process, for example the catalyst and the solvent.[21] The anisotropic short-range order is observed at the mesoscopic scale by X-ray and birefringence measurements. This is apparently governed by at least two different phenomena. The first one takes place in the solution during the formation of the Si–O–Si bonds by hydrolysis/polycondensation of the Si–OMe functions. The kinetics of each of these reactions and the possibility of interaction between the organic groups can each control the organisation of the molecular units at the molecular level. The second phenomenon takes place during the ageing of the gel. The continuation of the chemical processes (formation and redistribution of Si–O–Si) and elimination of the solvent leads to cracks in the gel and mechanical reorientation of the material. The anisotropic nanostructured hybrid materials that result are formed of a highly cross-linked Si–O–Si framework between non-mesogenic units. In other words this anisotropic behaviour is completely different from that of liquid crystals, which is controlled only by the van der Waals interactions between independent mesogenic units.

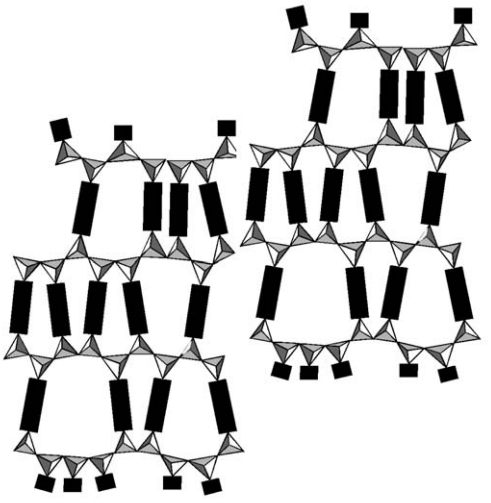

Scheme 1 Representation of an anisotropic organisation of an hybrid inorganic–organic xerogels with a rod-like rigid R group.

Such short-range organisation is fundamental for the development and application of these hybrid organic–inorganic materials. It is based to the possibility to control their physical and chemical properties due to co-operative interactions of the

organic groups. We thought it would be interesting to look at another determining parameter, the connectivity at silicon, corresponding to the number of cross-linkages (theoretical and experimental) on each silicon atom of a precursor. We chose to work with precursors **I–III**, which do not exhibit liquid crystal behaviour and do not require any catalyst to obtain solid formation.[22] This approach allows the preparation and comparison of a set of homologous solids since the organic group is the same in each, though with different connectivities at silicon. We prepared a linear polymer with a 1D structure from **III** (theoretical cross-linking level of 0) and covalent solids with a 3D structure for **I** and **II** (theoretical cross-linking levels of 1 and 2 at each silicon). Systems with $R[SiMe(OMe)_2]_2$ precursors have already been used,[23,24] but this is the first time that the possibility of self-organisation in these solids is reported. We also report the preparation of the crystallised polysiloxane prepared from **III**, which belongs to the main-chain polysiloxane family, some of which exhibit liquid crystal properties. Above all, the aim of this study is to test the effect of the interactions between organic moieties in the self-organisation of nanostructured hybrid organic–inorganic materials.

Experimental

All the reactions were carried out under a nitrogen atmosphere and solvents were dried before using according to already described procedures.[25]

^{29}Si NMR spectra were obtained on a Bruker AM300 at 59.620 MHz. Chemical shifts are given relative to tetramethylsilane. For CP MAS analyses, contact time was 2 ms, 10 s of recycle time, a spinning rate of 5 KHz, and acquisition of more than 1500 scans. Elemental analyses were performed by the Service Central de Microanalyse du CNRS.

Porosimetry measurements (specific surface area, pore diameter distribution and pore volumes) were conducted on a Micromeritics Gemini III and an ASAP 2010 porosimeter using high purity N_2 at −196 °C. Surface areas were calculated by the B.E.T. equation, micropore volumes using the t-plot and pore size distributions calculated using the Horvath–Kawazoe equation with a Saito–Foley cylindrical pore geometry.

Differential scanning calorimetry was performed on a DSC 6 Perkin Elmer analyser in aluminium cells in a stream of nitrogen (50 ml min^{-1}); the heating rate was 2 or 5 °C min^{-1}.

Observations by optical microscopy under polarised light were performed on materials prepared in a glass cell of 25 mm × 25 mm × 30 micron and coated with Teflon as reported previously.[18] Optical properties were measured with a Laborlux12POLS polarising microscope, photographs were taken using a Leica MPS28 camera. Measurement of the birefringence (Δn) was quantitatively made by equalising the index of refraction provoking the darkness of the bright zone with calibrated glass slides in order to determine Δl^*, $\Delta n = \Delta l^* \cdot d$ (d being the thickness of the gel that was taken equal to the thickness of the cell). Infrared analyses were performed on a Perkin Elmer 1600 FTIR analyser with samples being prepared in KBr pellets.

Precursor syntheses

Precursor I. This precursor was prepared according to the literature method.[22]

Precursor II. A solution of 5.40 g (20 mmol) of bis(trimethylsilylethynyl)benzene in 40 ml of dry tetrahydrofuran was prepared. Then the medium was cooled and kept at −40 °C. Methyllithium–lithium bromide complex, 31.4 ml (44 mmol) of 1.4 M solution in diethyl ether, was added dropwise to the solution. The white suspension obtained was warmed back slowly to room temperature followed by heating at 30 °C for 30 min. The appearance of the medium changed from translucent green to a grey suspension. The suspension was cooled once again to −50 °C, and transferred dropwise into a solution of 6.8 g (48 mmol) of chlorodimethoxymethylsilane dissolved in 40 ml of dry THF and kept at −70 °C. When all the lithium salt was added, the medium was warmed back slowly to room temperature and agitated for 15 h; a yellow translucent solution was obtained. This was evaporated under vacuum giving a yellow paste that was extracted by 15 ml of *n*-pentane and 10 ml of toluene (3 ×). Evaporation of all the solvents gave a viscous yellow syrup that was distilled under reduced pressure. Precursor **II** is obtained as a white solid at room temperature, b.p. 115–120 °C (0.07 mbar), m.p. 65 °C, yield 3.40 g (50%).^{1}H NMR in $CDCl_3$, δ (intensity): 7.48 (4.0), 3.66 (11.5), 0.36 (5.7). ^{29}Si NMR in $CDCl_3$, δ: −30.04.

Precursor III. This compound was prepared in the same way as for precursor **II** up through formation of the lithium salt. At this stage, the lithium salt is treated with 6.0 g (48 mmol) of chloromethoxydimethylsilane dispersed in 40 ml of dry THF cooled and kept at −70 °C. The suspension of lithium salt was cooled to −50 °C and transferred dropwise into the chlorosilane solution. When all the lithium salt was added, the medium was warmed back slowly to room temperature and agitated for 15 h. A yellow translucent solution was obtained and evaporated under vacuum, which led to the formation of a yellow paste. The paste was extracted by 15 ml of *n*-pentane and 10 ml of toluene (3 ×), followed by evaporation of all the solvents. The viscous yellow oil that remained was distilled under reduced pressure. Precursor **III** was obtained as a white solid, m.p. 80 °C, b.p. 90–95 °C (0.04 mbar), yield 3.50 g (57%).^{1}H NMR in $CDCl_3$, δ (intensity): 7.45 (4.0), 3.58 (5.7), 0.35 (12.2).^{29}Si NMR in $CDCl_3$, δ: −7.66.

General procedure for the synthesis of the xerogels

Gellations were all carried out at room temperature without any catalyst. To achieve a homogeneous reaction medium, the precursor and a solvent were mixed to form the solution 1. Separately, water was diluted with the same solvent in another glass tube to form solution 2. Then solution 2 was added rapidly to solution 1 and the mixture was stirred vigorously under nitrogen for 2 min. The proportions of solutions 1 and 2 varied in agreement with the values given below. A slight amount of this mixture was put into the glass cell, which was used for microscopic observation and measurement of the birefringence. The remaining solution was allowed to rest in order for gellation to occur. The gel was then allowed to stand for 1 week and then crushed, washed with acetone (20 ml), diethyl ether (20 ml) and finally dried for 12 h at 100 °C under vacuum (0.1 mm Hg). Yields of these preparations were sometimes over 100% due to the presence of remaining Si–OR (R = H or Me) groups or slight residues of solvents.

Xerogel HM_{Ia}. The mixture for gellation was made with 1.04 g (2.84 mmol) of **I**, 0.15 g (8.52 mmol) of water and 2.70 ml of tetrahydrofuran. The sol was transparent and the gelation time was 21 min. Syneresis started after 1 day. A hard xerogel was obtained, 0.64 g (yield 99%).

Xerogel HM_{Ib}. The mixture for gellation was made with 1.10 g (3.00 mmol) of **I**, 0.16 g (9.00 mmol) of water and 2.84 ml of methanol. The sol was translucent. Gelation time was 8 min and syneresis started after 12 h (contraction of the gel). A soft and light xerogel was obtained, 0.69 g (yield 99%).

Xerogel HM_{Ic}. The mixture for gellation was made with 1.10 g (3.00 mmol) of **I**, 0.16 g (9.00 mmol) of water and 2.84 ml of acetonitrile. The sol was transparent and gellation occurred within 1 min. Syneresis started after 30 min and it shrank strongly. A light xerogel was obtained, 0.65 g (yield 95%).

Xerogel HM_{IdId}. The mixture for gellation was made with 0.78 g (2.13 mmol) of **I**, 0.11 g (6.39 mmol) of water and 2.01 ml of acetone. The sol was transparent and gellation time was 55 min. Syneresis started after 1 day and it slowly shrank. A soft xerogel was obtained, 0.49 g (yield 101%).

Xerogel HM_{Ie}. The mixture for gellation was made with 0.88 g (2.40 mmol) of **I**, 0.13 g (7.22 mmol) of water and 2.27 ml of toluene. After 6 min, precipitation was observed and the medium became heterogeneous. Syneresis started after half a day but was difficult to precisely determine. A soft and light xerogel was obtained, 0.51 g (yield 93%).

Xerogel HM_{IIa}. The mixture for gellation was made with 1.01 g (3.02 mmol) of **II**, 0.109 g (6.04 mmol) of water and 2.91 ml of tetrahydrofuran. The sol was transparent and gellation time was 50 min. Syneresis started after 2 days. A hard and light xerogel was obtained, 0.64 g (yield 87%).

Xerogel HM_{IIb}. The mixture for gellation was made with 0.66 g (1.98 mmol) of **II**, 0.07 g (3.96 mmol) of water and 1.92 ml of methanol. The sol became opaque. Gellation time was 22 min, while the medium was heterogeneous. Syneresis started after 1 day though it was not easy to precisely determine. A hard and light xerogel was obtained, 0.48 g (yield 99%).

Xerogel HM_{IIc}. The mixture for gelation was made with 0.77 g (2.30 mmol) of **II**, 0.08 g (4.60 mmol) of water and 2.22 ml of acetonitrile. The sol was translucent and gelation occurred within 2 min. Syneresis started after 6 min and the gel shrank dramatically. A hard and dense xerogel was obtained, 0.54 g (yield 97%).

Xerogel HM_{IId}. The mixture for gelation was made with 0.96 g (2.87 mmol) of **II**, 0.10 g (5.74 mmol) of water and 2.77 ml of acetone. The sol was transparent and gelation time was 80 min. Syneresis started after 2 days and the gel gradually shrank. A hard xerogel was obtained, 0.61 g (yield 88%).

Xerogel HM_{IIe}. The mixture for gelation was made with 0.90 g (2.69 mmol) of **II**, 0.09 g (5.38 mmol) of water and 2.59 ml of toluene. After 13 min, colloid precipitation was observed and the syneresis phenomenon became heterogeneous. Syneresis started after 1 day and it was slight. A hard and light xerogel was obtained, 0.65 g (yield 99%).

Polymer HM_{III}

A mixture of 1.07 g (3.52 mmol) of **III**, 0.06 g (3.52 mmol) of water and 3.46 ml of tetrahydrofuran was prepared at room temperature. The solution was transparent, but after 2 days, small white grains and short needles started to form. The average diameter of the grains was 1.0–1.5 mm and the average length of the needle-shaped crystals was 1.5–2.0 mm. By evaporating the solvent, a pale orange powder was obtained, 0.86 g (yield 95%) ^{1}H NMR in $CDCl_3$, δ (intensity): 7.45 (4.00), 3.58 (0.22), 0.35 (11.9). ^{29}Si NMR in $CDCl_3$, δ (intensity): −7.66 (0.01), −13.8 (0.06), −16.9 (1.00), −17.9 (0.07), −19.1 (0.06).

Results

Hybrid materials HM_I

The gellation of **I** was performed in different solvents according to Scheme 2. In all the cases the gellation times were generally short (Table 1). The time necessary for the syneresis to start is also given since the syneresis evidences the contraction and reorganisation of the framework.

The initial solutions were completely transparent in normal light, and dark when observed by optical microscopy in polarised light. This is also the case when the gel starts to form. This reveals an isotropic medium in both cases. Ageing of the wet gels leads, after 1 or 2 h, to the formation of cracks, initially on the edges of the cell where evaporation of the solvent is relatively fast. The cracking of the gel, and especially the number and orientation of the cracks, depends on the solvent. However, these observations are purely qualitative at the present time and cannot be quantified.

In all cases, birefringent pieces of HM_{Ia-e} result from the cracking of the gel. Examples are given in Fig. 1 and 2. These pieces of solids can be considered as xerogels although they may not be completely dry. The average value of the birefringence

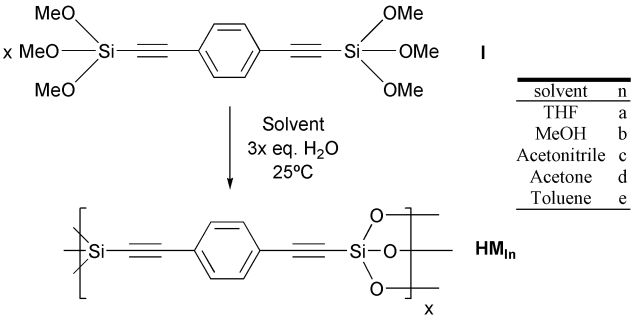

Scheme 2 Preparation of the HM_{In} xerogels **I**.

Table 1 Characteristics of hybrid xerogels HM_{Ia-e}

Xerogel	Solvent	Gelation/min (start of syneresis/h)	$T^{1\,a}$ (%)	$T^{2\,a}$ (%)	$T^{3\,a}$ (%)	DC^b	Cross-linking level (Si–O–Si/Si)	Birefringence value/10^{-3}	Specific surface area/m^2 g^{-1}	Porosity
HM_{Ia}	THF	21 (24)	15	47	38	74	2.2	2.9	120	Microporous
HM_{Ib}	MeOH	8 (12)	16	54	30	71	2.1	2.3	840	Micro- and meso-porous
HM_{Ic}	CH_3CN	1 (0.5 strong)	8	57	35	75	2.2	2.4	780	Microporous
HM_{Id}	Acetone	55 (24)	10	58	32	74	2.2	2.8	670	Microporous
HM_{Ie}	Toluene	6 (12)	10	61	29	73	2.1	2.4	650	Microporous

^{a} Relative percentage. ^{b} Degree of polycondensation calculated according to the general equation DC = [0.5(T^1 area) + 1.0(T^2 area) + 1.5(T^3 area)]; T^1 [C–*Si*(OR)$_2$–(O–Si)], T^2 [C–*Si*(OR)–(O–Si)$_2$], T^3 [C–*Si*(O–Si)$_3$].

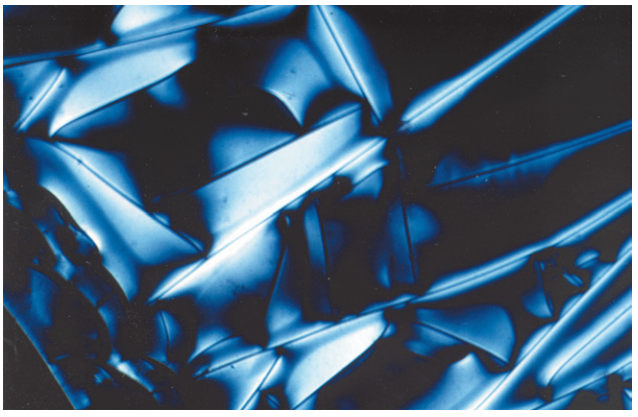

Fig. 1 Xerogels $\mathbf{HM_{Ia}}$.

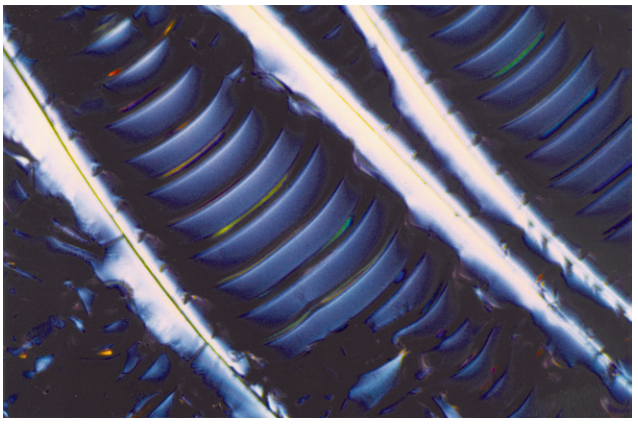

Fig. 2 Xerogels $\mathbf{HM_{Ib}}$ from precursor **I**.

determined in different areas of the cell are around $2.6 \pm 0.3 \times 10^{-3}$; these values remain unchanged even after several weeks (Table 1). Depending on the nature of the solvent, the birefringence varies from 10 to 15%, this suggests a low effect of the solvent on the birefringence of xerogels prepared from **I**.

The textural characteristics of these materials were obtained by porosimetry measurements with nitrogen (Table 1). In contrast to the birefringence, a drastic solvent effect is now observed. Microporous materials with a specific surface area as low as 120 $m^2\ g^{-1}$ (THF) or (micro + meso)porous materials with a specific surface area as high as 840 $m^2\ g^{-1}$ (MeOH) are formed, depending on the solvent. Therefore, variation of the texture apparently has connections with the solvent but not with the birefringence intensity.

By ^{29}Si NMR spectroscopy we found that the degree of condensation (DC) is generally high as indicated by the presence of T^1, T^2 and T^3 signals[26] (Table 1). CP MAS spectroscopy is a fast method but sometimes not quantitative for analysing these materials, especially because silicon atoms corresponding to T^3 units that are far away from any proton leads to very slow relaxation processes. Thus, the values of the degree of condensation (DC) determined by looking at the relative intensity of the $T^1/T^2/T^3$ signals are always qualitative and underestimated. In these conditions, the level of condensation was found to lie in the same range for all the HM_{Ia-e} solids (at least $\geqslant 71\%$) and corresponds to an average >2.2 Si–O–Si links per silicon atom (Table 1). This qualitative comparison of the DC of HM_{Ia-e} solids suggests that for solids prepared from **I**, the level of condensation is only weakly dependent on the nature of the solvent, just like the birefringence intensity.

DSC analysis shows two transformations for HM_{Ia} [Fig. 3(a)]. The first one from 50 to 150 °C is endothermic, probably due to the elimination of solvent adsorbed on the solid or elimination of water that forms by condensation of residual silanols. The second phenomenon is exothermic from

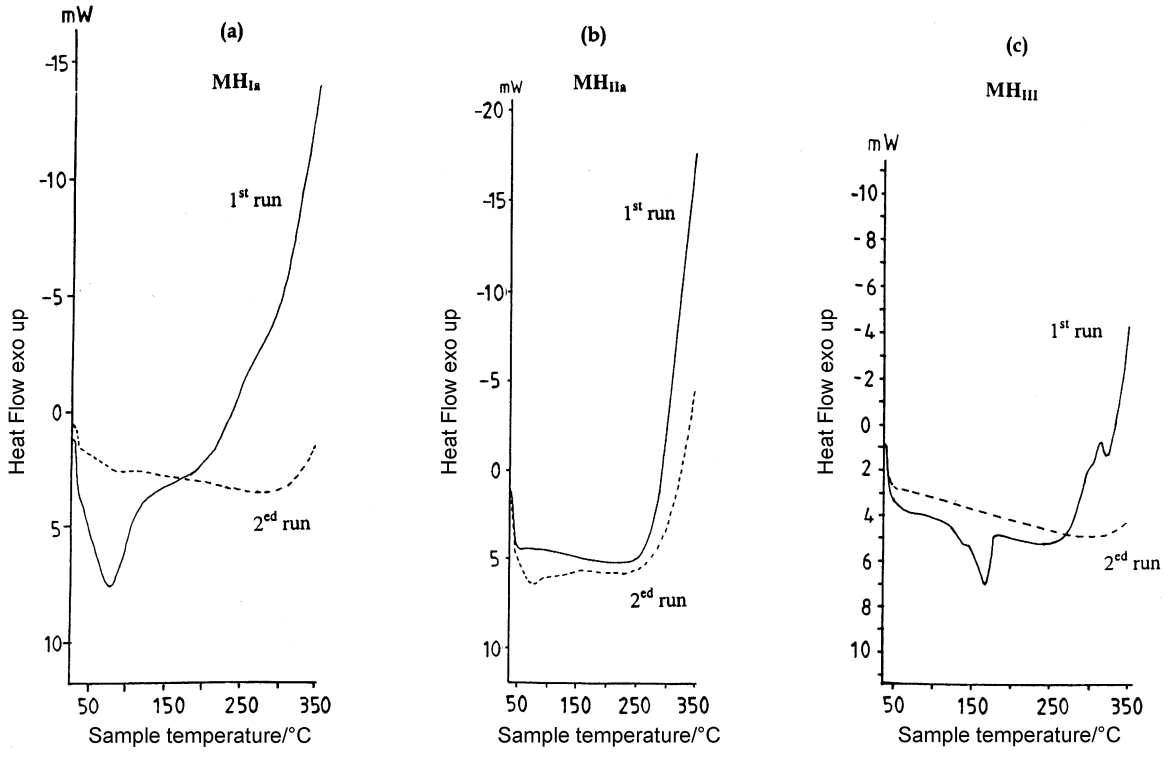

Fig. 3 Differential scanning calorimetry analyses of (a) $\mathbf{HM_{Ia}}$, (b) $\mathbf{HM_{IIa}}$ and (c) $\mathbf{HM_{III}}$ from 25 to 350 °C in aluminium cells and under nitrogen.

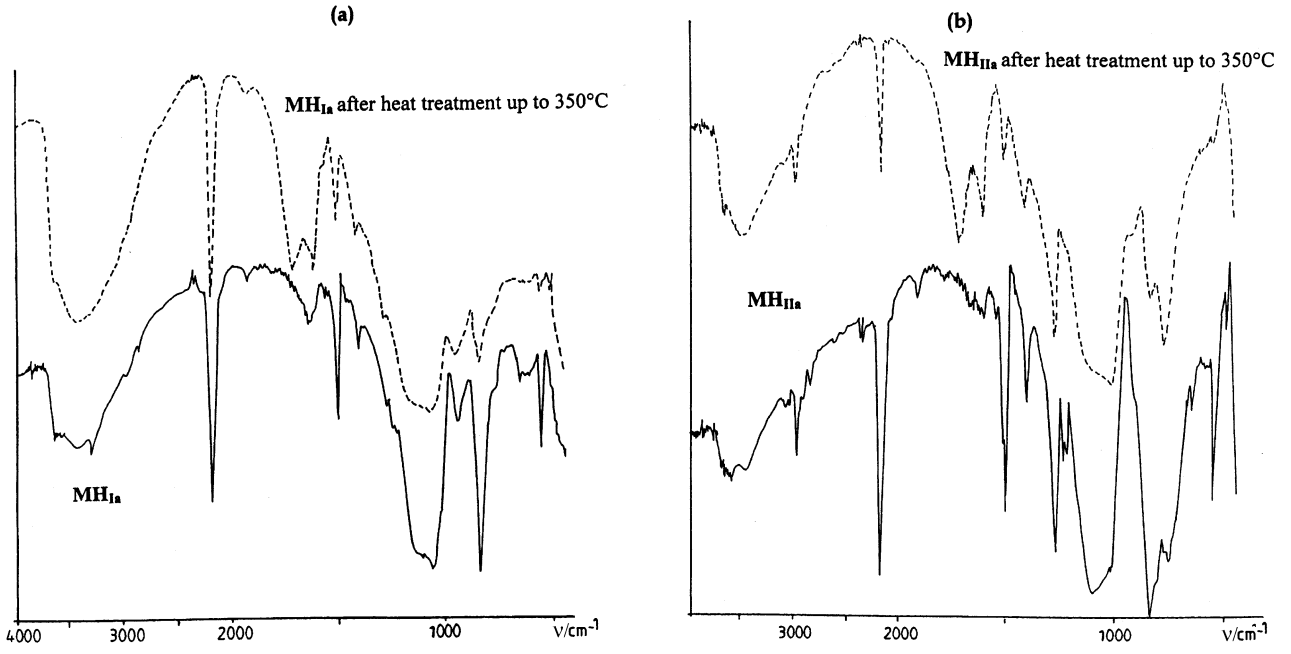

Fig. 4 IRTF analyses analyses in KBr pellets of (a) $\mathbf{HM_{Ia}}$ and (b) $\mathbf{HM_{IIa}}$

220 up to 350 °C. It is attributed to the cross-linking between the organic units by reaction between the acetylenic groups. Indeed, infrared analysis indicates, after thermal treatment, a decrease of the signal attributed to C≡C groups ($\nu = 2170$ cm^{-1}) and the presence of new signals attributed to C=C conjugated systems [$\nu = 1716$ and 1607 cm^{-1}; Fig. 4(a)]. It was also evident that a majority of the C≡C bonds did not react at this temperature (350 °C), certainly because of the high level of cross-linking of the materials, which limits the movements and interactions of the units. When a second DSC analysis was performed on the same sample, no exothermic phenomenon was observed and the infrared spectrum was essentially unchanged. The lack of reactivity of the remaining acetylenic group may be attributed to the high level of cross-linking, which prevents deformations of the solid architecture favourable to the reaction of the acetylenic groups.

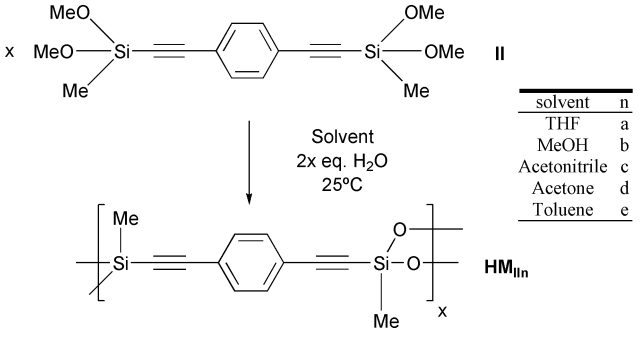

Scheme 3 Preparation of the $\mathbf{HM_{IIn}}$ xerogels **II**.

Hybrid materials $\mathbf{HM_{II}}$

The gellation of **II** was also performed in different solvents according to Scheme 3. Gellation and syneresis times were also short and suggest a high reactivity of this precursor, as for **I** (Table 2). The same process of gellation, ageing and cracking was observed as for gels and xerogel from **I** (*vide supra*). After cracking, all the pieces of HM_{IIa-e} xerogels were found to be birefringent in all cases (Fig. 5 and 6). However, the birefringence of HM_{IIa-e} is a little higher than for HM_{Ia-e}, moreover, it depends on the solvent in contrast to that of HM_{Ia-e}. The birefringence value ranged from 2.7 to 5.6×10^{-3}, depending on the solvent. For HM_{IIb} prepared in methanol a precipitation phenomenon prevents any measurement; a white solid forms and its birefringence cannot be determined.

Textural analyses of theses HM_{IIa-e} revealed that most of them are less porous than HM_{In}, a porous solid being obtained with a specific surface area of up to 670 m^2 g^{-1} (CH_3CN) only in the case of HM_{IIc}. In addition, macro- and/or mesopores were observed here but never micropores. From a general

Table 2 Characteristics of hybrid xerogels HM_{IIa-e}

Xerogel	Solvent	Gelation/min (start of syneresis/h)	D^1 [a] (%)	D^2 [a] (%)	DC[b]	Cross-linking level (Si–O–Si/Si)	Birefringence value/10^{-3}	Specifique surface area/m^2 g^{-1}	Pore characteristics
HM_{IIa}	THF	50 (48)	38	62	81	1.6	5.6	<10	—
HM_{IIb}	MeOH	22 (24)	60	40	70	1.4	—	<10	—
HM_{IIc}	CH_3CN	2 (0.1 strong)	26	74	88	1.7	3.1	670	Macro and meso
HM_{IId}	Acetone	80 (48)	23	77	89	1.8	3.9	200	Meso and micro
HM_{IIe}	Toluene	13 (24)	22	78	90	1.8	2.7	340	Macro and meso

[a] Relative percentage. [b] Degree of polycondensation according to the general equation $DC = [0.5(D^1 \text{ area}) + 1.0(D^2 \text{ area})]$; D^1 [C–*Si* $(OR)_2$–(O–Si)], D^2 [C–*Si*(OR)–$(O–Si)_2$].

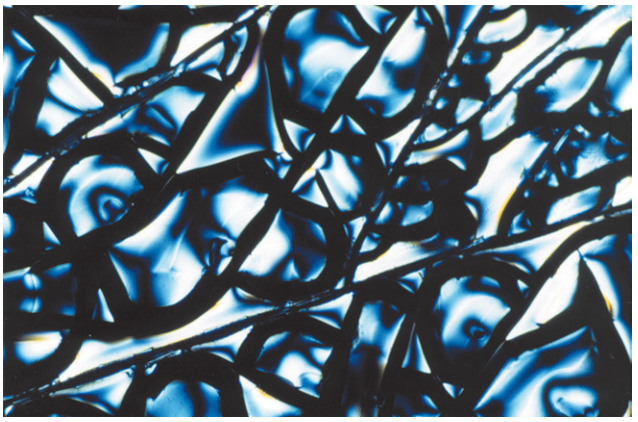

Fig. 5 Xerogels $\mathbf{HM_{IIa}}$ from precursor **II**.

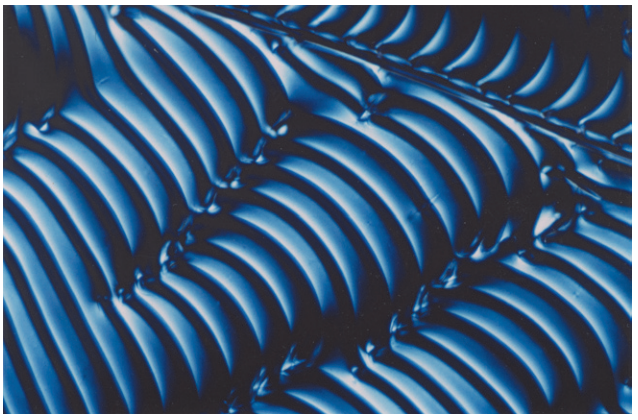

Fig. 6 Xerogels $\mathbf{HM_{IIb}}$ from precursor **II**.

point of view, like for the preparation of MH_{Ia-e} solids, the role of the solvent on the texture of HM_{IIa-e} solids is important. But in addition, in the case of HM_{IIa-e}, the solvent has an effect on the birefringence.

By ^{29}Si NMR spectroscopy D^1 and D^2 signals were observed with chemical shift agreeing with the previous literature (Table 2).[26] No T^n units were observed, indicating the absence of Si–C*sp* bonds cleavage. We checked the degree of condensation (DC) of HM_{IIa-e}, but like for HM_{Ia-e} and for the same reasons, the DC is certainly underestimated and is given as a minimum value. Qualitatively, DC is high, in agreement with previous data on $R[Si(Me)O_{1,5}]_2$ solids.[24] In contrast to HM_{Ia-e}, variation of DC is observed for MH_{IIa-e} depending on the solvent. A tentative comparison of HM_{IIa} and HM_{Ia} suggests that the level of polycondensation of HM_{IIa} is higher than for HM_{Ia}; however, the level of cross-linking (number of Si–O–Si per silicon atom), corresponds to an average of 1.8 Si–O–Si/Si for HM_{IIa} and 2.2 Si–O–Si/Si for HM_{Ia}. It also appears that a decrease of the level of condensation corresponds with an increase of the birefringence (Table 2).

When analysed by DSC analysis [Fig. 3(b)], HM_{IIa} exhibits the same endothermic phenomenon as that of MH_{Ia} from 50 to 150 °C, due to the loss of residual solvent and loss of water from condensation of residual silanols. When increasing the temperature an exothermic phenomenon starting at 270 °C was measured and attributed again to the reaction of the acetylenic group. This was confirmed by the infrared spectrum. After heat treatment we observed a decrease of the signal attributed to C≡C groups ($\nu = 2170$ cm^{-1}) and the presence of new signals attributed to C=C conjugated systems [$\nu = 1716$ and 1607 cm^{-1}; Fig. 4(b)]. However, the thermal behaviour of both HM_{IIa} and HM_{Ia} are not precisely the same: reaction of HM_{IIa} starts at a higher temperature and the decrease of the acetylenic signal intensity is higher. Moreover, when the sample is analysed a second time, the exothermic phenomena is not observed for MH_{Ia} while it is observed again for MH_{IIa}, although with a lower intensity. A possible reason might be the lower degree of cross-linking in MH_{IIa}corresponding to fewer links and a more mobile Si–O–Si network upon heating, thus allowing the acetylenic group to react at a lower temperature and also during the second step.

Polymer HM_{III}

Hydrolysis-polycondensation of **III** was performed in THF according to Scheme 4 and the analyses agree with the formation of a polymeric material. ^{29}Si NMR analysis in solvent presents mainly one signal at −16.9 ppm corresponding to the repetitive units –(–O–$SiMe_2$–C≡C–C_6H_4–C≡C–$SiMe_2$–)– of the polymer. A signal of very low intensity at −7.66 ppm indicates the presence of remaining $Si(OMe)_3$ groups by comparison to the starting precursor; other signals of very low intensity at −13.8, −17.9, −19.1 ppm could be attributed to hydrolysed but not polycondensed –$SiMe_2$(OH) groups at the end of the chains or to cyclic dimers. By ^{1}H NMR analysis, the intensity of the Si–OMe signal is very weak and not useful for integration. By SEC (size exclusion chromatography) analysis an average molecular weight of 15 500 g mol^{-1} was determined and corresponds to a degree of polymerisation DP_n of 60 (MW of the unit chain is 250 g mol^{-1}). However, this result must be taken as an estimation since the rod-like shape of the molecular units of this polymer is very different from that of the polystyrene used for calibration of the SEC apparatus.

Upon slow evaporation of the solvent, the solid polymer crystallises from the solution and forms spherolites that grow in the cell (Fig. 7). Their birefringence is very high at 25.3, and their shape clearly indicates a crystallised polymer with a well-defined organisation.

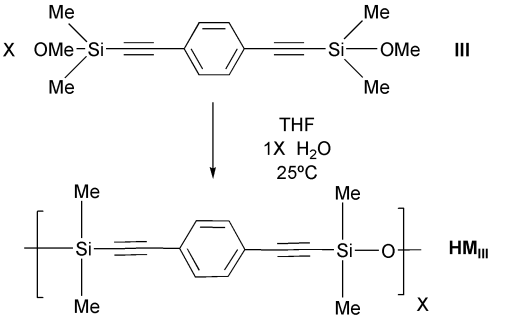

Scheme 4 Preparation of $\mathbf{HM_{III}}$.

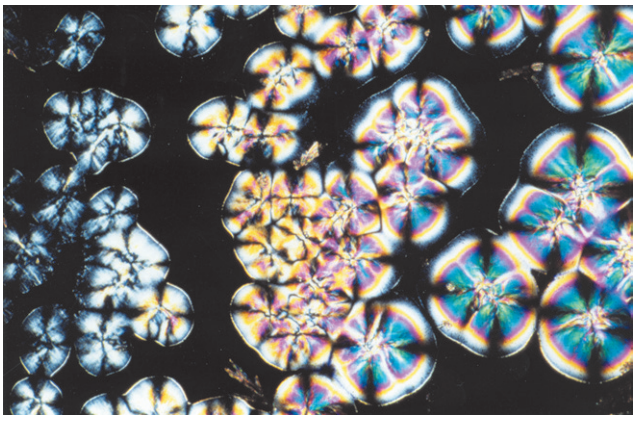

Fig. 7 $\mathbf{HM_{III}}$ from precursor **III**.

When analysed by DSC, HM_{III} exhibits two endothermic phenomena centred at 142 and 167 °C [Fig. 3(c)]. The latter corresponds to the melting point of the polymer and the former may be attributed *a priori* to a phase transition suggesting a liquid crystal behaviour (more studies are in progress to determine the organisation of the solid and its liquid crystal properties). When heated to higher temperature an exothermic phenomena starts at 270 °C. As in the case of $HM_{IIa}$and HM_{Ia} this is attributed to acetylenic reaction and is confirmed by infrared analysis.

Discussion

Changing the connectivity at silicon [Si(OMe)/Si = 3 for **I**, = 2 for **II**, = 1 **III**] provides information on the formation of the short-range organisation of hybrid organic-inorganic materials. Comparison of HMn_{a-e} (n = **I**, **II** and **III**) materials and of their reactivity leads to results that confirmed our previous work.[18,20,21] First, the organisation at the molecular level occurs during hydrolysis/polycondensation (at the sol step) and it is based on the Van der Waals interactions between organic groups. Secondly, the development of this organisation into micrometer size domains is due to the reorganisation and reorientation produced during the cracking of the gel.

The first hypothesis is confirmed by the behaviour of polymer HM_{III} demonstrating the ability of these systems to self-organise. This polymer, with an organic group that is used for the other hybrid materials HM_{Ia-e} and HM_{IIa-e}, exhibits excellent crystalline organisation, which illustrates the ability of –(SiR′R″–C≡C–C_6H_4–C≡C–SiR′R″–O–) units to self-organise. Although the packing of the chains and the arrangement of their molecular units are still under investigation, it is clear that the organisation of the solid polymer HM_{III} results from a thermodynamic process corresponding to the Van der Waals interactions between the organic groups and formed upon evaporation of the solvent. In contrast, organisation of HM_{Ia-e} and HM_{IIa-e} is mainly irreversible once the Si–O–Si bonds start to form and cross-link the system. Therefore, the self-organisation is not achieved so nicely compared to HM_{Ia-e}. Additionally, the possibility to polymerise the acetylenic groups of the solids HM_{Ia-e} and HM_{IIa-e} are arguments for a self-organisation process. Indeed, as in the case of the polymerisation of the diacetylenic units of $O_{1.5}$Si–CC–CC–$SiO_{1.5}$ xerogels previously reported,[27] such polymerisation probably requires a precise positioning of the acetylenic units between each other. We note that there are few examples of thermally activated solid-state reactions between acetylenic units.[28] The lower thermal reactivity of the HM_{II} compared to HM_{I} may be attributed to steric hindrance of Si–Me groups. As a result of this chemical transformation, cross-linking between the organic units occurs and the formation of structures like in Scheme 5 can be proposed.

The second hypothesis concerns the anisotropic organisation on large domains (micrometric scale) occurring when the gel is formed and has started to crack. It clearly appears related to the connectivity at silicon. The behaviour of HM_{Ia-e} and HM_{IIa-e} illustrate the close relationship between the stress/relaxation process and the level of polycondensation. HM_{IIa-e}, which are less polycondensed than HM_{Ia-e}, are more sensitive to this process and more dependent on the experimental conditions than HM_{Ia-e}. Furthermore, because HM_{Ia-e} are more cross-linked, they are less dependent on the experimental conditions, but the xerogels are also less birefringent. Thus, it appears that at the ageing step, when cracking of the gel occurs due to its chemical evolution (loss of solvent, contraction due to Si–O–Si formation and redistribution),[29] the reorientation process is favoured by the less cross-linked HM_{IIa-e} compared to MH_{Ia-e}. However, we stress that the level of cross-linking is determined both by the nature of the precursor but also by the chemistry at work during all these processes.

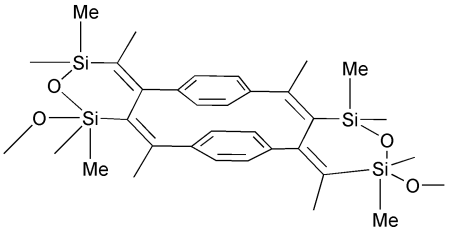

Scheme 5 Representation of the formation of two acetylenic-polymerized precursors units upon heat treatment of $\mathbf{HM_{IIa}}$ at 350 °C.

Conclusion

Nanostructured silicon-based hybrid materials of general formula $O_{1.5(3-n)}SiMe_n$–C≡C–C_6H_4–C≡C–$SiMe_nO_{1.5(3-n)}$ (n = 0, .1, 2) are anisotropic materials. The present results stress that their short-range organisation is extended over several micrometers and is the combination of two processes, the self-association between the macromolecular species at the sol step and the reorientation process during the ageing step of the gel.

From a general point of view, a control of the organisation of silicon-based hybrid material prepared by sol–gel chemistry can be achieved by combining a control of both the chemical processes at the molecular level and the physical evolution.

Acknowledgements

The authors are grateful to Silicones Electronics Materials Research Center from ShinEtsu Chemical Co.

References

1 D. A. Loy and K. J. Shea, *Chem. Rev.*, 1995, **95**, 1431.
2 K. J. Shea and D. A. Loy, *Mater. Res. Bull.*, 2001, **5**, 358.
3 R. J. P. Corriu and D. Leclecq, *Angew. Chem., Int. Ed. Engl.*, 1996, **35**, 4001.
4 R. J. P. Corriu, *Angew. Chem., Int. Ed.*, 2000, **39**, 1376.
5 B. Boury and R. J. P. Corriu, in *The Chemistry of Organic Silicon Compounds*, eds. Z. Rappoport and Y. Apeloig, Wiley & Sons, Chichester, UK, 2000, p. 565.
6 E. Toussaere, J. Zyss, P. Griesmar and C. Sanchez, *Nonlinear Optics*, 1991, **1**, 349.
7 Z. Yang, C. B. Xu, L. R. Dalton, S. Kalluri, W. H. Steier and J. H. Bechtel, *Chem. Mater.*, 1994, **6**, 1899.
8 R. J. P. Corriu, P. Hesemann and G. Lanneau, *Chem. Commun.*, 1996, 1845.
9 B. Lebeau, S. Brasselets, J. Zyss and C. Sanchez, *Chem. Mater.*, 1997, **9**, 1012.
10 A.-C. Franville, D. Zambon and R. Mahiou, *Chem. Mater.*, 2000, **12**, 428.
11 A. C. Franville, D. Zambon, R. Mahiou, S. Chou, Y. Troin and J. C. Cousseins, *J. Alloys. Compd.*, 1998, **275–277**, 831.
12 Y. Lu, H. Fan, N. Doke, D. Loy, R. A. Assink, D. A. LaVan and C. J. Brinker, *J. Am. Chem. Soc.*, 2000, **122**, 5258.
13 M. J. MacLachlan, T. Asefa and G. Ozin, *Chem. Eur. J.*, 2000, **6**, 14.
14 T. Asefa, C. Yoshina-Ishii, M. J. MacLachlan and G. A. Ozin, *J. Mater. Chem.*, 2000, **10**, 1751.
15 A. Shimojima, Y. Sugahara and K. Kuroda, *J. Am. Chem. Soc.*, 1998, **120**, 4528.
16 J. J. E. Moreau, L. Vellutini, M. Wong Chi Man and C. Bied, *J. Am. Chem. Soc.*, 2001, **123**, 1509.
17 J. J. E. Moreau, L. Vellutini, M. Wong Chi Man, C. Bied, J.-L. Batignies, P. Dieudonné and J.-L. Sauvajol, *J. Am. Chem. Soc.*, 2001, **123**, 7957.
18 B. Boury, R. J. P. Corriu, P. Delord, M. Nobili and V. Le Strat, *Angew. Chem., Int. Ed.*, 1999, **38**, 3172.
19 B. Boury, R. J. P. Corriu, P. Delord and V. Le Strat, *J. Non-Cryst. Solids*, 2000, **265**, 41.

20 F. Ben, B. Boury, R. J. P. Corriu and V. Le Strat, *Chem. Mater.*, 2000, **12**, 3249.
21 B. Boury, F. Ben, R. J. P. Corriu, P. Delord and M. Nobili, *Chem. Mater.*, 2002, **14**, 730.
22 P. Chevalier, R. J. P. Corriu, P. Delord, J. J. E. Moreau and W. C. H. Man, *New J. Chem.*, 1998, **22**, 423.
23 E. Lindner, T. Scheller, F. Auer and H. A. Mayer, *Angew. Chem., Int. Ed.*, 1999, **38**, 2154.
24 A. L. Loy, G. M. Jamison, B. M. Baugher, S. A. Myers, R. A. Assink and K. J. Shea, *Chem. Mater.*, 1996, **8**, 656.
25 A. J. Gordon and R. A. Ford, *The Chemist's Companion*, Wiley, New York, 1972.
26 H. Marsmann, in *NMR Basic Principles and Progress*, eds. P. Dielh, E. Fluck and R. Kosfeld, Springer Verlag, Berlin, 1981, vol. 17, p. 65.
27 R. J. P. Corriu, J. J. E. Moreau, P. Thepot and M. Wong Chi Man, *Chem. Mater.*, 1996, **8**, 100.
28 K. Tanaka and F. Toda, *Chem. Rev.*, 2000, **100**, 1025.
29 C. J. Brinker and G. W. Scherer, *Sol-Gel Science*, Academic Press, Inc., Boston, 1990.